



ELSEVIER

Journal of Computational and Applied Mathematics 103 (1999) 67–76

JOURNAL OF
COMPUTATIONAL AND
APPLIED MATHEMATICS

Numerical simulation of flow past a sphere in vertical motion within a stratified fluid

Carlos R. Torres^{a,*}, José Ochoa^b, José E. Castillo^c, Hideshi Hanazaki^d

^a*Oceanografía Física, Instituto de Investigaciones Oceanológicas, U.A.B.C., A.P. 453, 22800, Ensenada B.C., Mexico*

^b*Oceanografía Física, Centro de Investigación Científica y de Educación Superior de Ensenada. Km. 107 Carr. Tij-Eda. Ensenada B.C., Mexico*

^c*Department of Mathematics, San Diego State University, San Diego, CA 92182-0314, USA*

^d*Institute of Fluid Science, Tohoku University 2-1-1, Katahira, Aoba-Ku, Sendai 980-77, Japan*

Received 17 May 1997; received in revised form 11 February 1998

Abstract

In the present study we consider a viscous fluid, stratified by a diffusive saline agent and compute numerically the flow produced by a solid sphere moving vertically and uniformly. The governing equations describing this situation are solved on a variational grid. The results show the dependence of the boundary-layer separation point and the vanishing of vortices behind the sphere as the stratification increases at moderate Reynolds number flows. Details of the flow, density and pressure fields near the sphere are also shown. Important quantities for engineering use (drags, pressure and skin coefficients) are also computed and displayed in the Richardson vs. Reynolds number space. Comparison with experimental evidence shows an excellent agreement. © 1999 Elsevier Science B.V. All rights reserved.

Keywords: Viscous flow; Variational grids; Flow past sphere

Notation

| | |
|------------------------|-----------------------------------|
| ρ, ρ_0, ρ_e | density |
| κ | mass diffusivity coefficient |
| ν | kinematic diffusivity coefficient |
| F | Froude number |
| Re | Reynolds number |
| Sc | Schmidt number |

* Corresponding author.

| | |
|-------------------------|------------------------------------|
| N^2 | Brunt–Vaisala frequency |
| p, p_e | pressure |
| $\hat{p}, \hat{\rho}$ | pressure and density perturbations |
| g | acceleration due to gravity |
| t | time |
| a | radius of the sphere |
| z, r | spatial coordinates |
| W, w, u | velocity components |
| ξ, η | transformed coordinates |
| J | Jacobian of the transformation |
| α, β, γ | metrics of the transformation |

1. Introduction

The behaviour of stratified fluids around objects has been studied both theoretically and experimentally during many years. Such flows display many remarkable phenomena not present in the homogeneous case. In the homogeneous case, the separation of the Boundary Layer (*BL*) is associated with a recirculating zone behind the object and occurs for Reynolds numbers as low as 40 for spheres (see for example, plate 3 in [1]). In the case of a vertically moving sphere in a stratified fluid Ochoa and Van Woert [2] have observed that even for high Reynolds numbers, depending on the strength of the stratification, the *BL* remains attached to the sphere up to the pole where a thin wake is left behind. In order to produce recirculating cells with a *BL* separation before the pole, higher *Res*, as compared with the homogeneous case, must be reached (see Fig. 106 in [6]). In order to reproduce the above observations, in this study the Navier–Stokes equations are solved numerically to describe the steady flow caused by a sphere moving vertically at a constant speed in a linearly stratified Boussinesq fluid. The fluid is viscous and the density is diffusive. Fig. 1 shows the schematics of the flow problem.

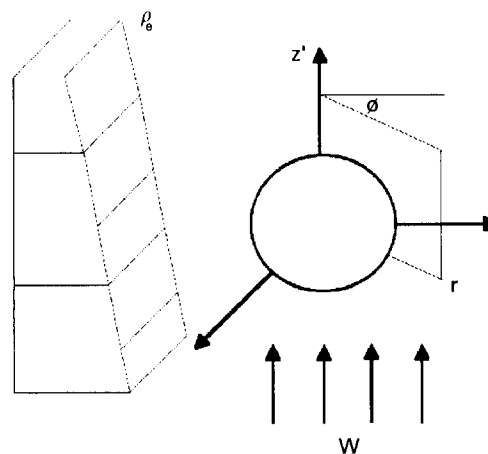


Fig. 1. Schematics of the flow problem.

2. Equations of motion

The governing Navier–Stokes equations describing a viscous stratified diffusive flow are

$$\frac{D\mathbf{u}}{Dt} = -\frac{1}{\rho_0} \nabla p + \frac{\rho}{\rho_0} \mathbf{g} + \nu \nabla^2 \mathbf{u}, \quad (1)$$

$$\frac{D\rho}{Dt} = \kappa \nabla^2 \rho, \quad (2)$$

$$\nabla \cdot \mathbf{u} = 0, \quad (3)$$

where the Boussinesq and incompressibility approximations have been included and (2) is the heat or salinity equation in terms of density. If we consider a basic hydrostatic state from a moving frame of reference, then the density and pressure fields are given, respectively, by

$$\rho_e = \rho_0 + \frac{\partial \rho_e}{\partial z} (z - Wt), \quad (4)$$

$$\nabla p_e = \rho_e \mathbf{g}. \quad (5)$$

If $\hat{\rho}$ and \hat{p} denote the deviations of density and pressure from the basic state, then

$$\rho = \rho_e + \hat{\rho}, \quad (6)$$

$$p = p_e + \hat{p}. \quad (7)$$

Inserting (6) and (7) in (1)–(3) and subtracting the basic state, the equations in dimensionless form are written as follows:

$$\frac{D\mathbf{u}}{Dt} = -\nabla \hat{p} + \frac{\hat{\rho}}{F^2} \mathbf{j} + \frac{2}{Re} \nabla^2 \mathbf{u}, \quad (8)$$

$$\frac{D\rho}{Dt} = (1 - w) + \frac{1}{Re Sc} \nabla^2 \hat{\rho}, \quad (9)$$

where velocities have been scaled by the exterior velocity (W), distances by the radius of the sphere (a), pressure perturbation by $\rho_0 W^2$ and density perturbation by $a \partial \rho_e / \partial z$. The dimensionless Reynolds, internal Froude and Schmidt numbers, are given by

$$Re = \frac{2Wa}{\nu}; \quad F = \frac{W}{Na}; \quad Sc = \frac{\nu}{\kappa},$$

where

$$N^2 = -\frac{g}{\rho_0} \left(\frac{\partial \rho_e}{\partial z} \right)$$

is the buoyancy frequency. In this study, we used $Sc = 700$ corresponding to stratification made by salt. Hereafter the ($\hat{\cdot}$) are dropped and thus perturbed variables are used in the next equations.

In the primitive variable formulation (8)–(9) is solved in conjunction with a Poisson equation for the pressure which is obtained by taking the divergence of (8). Hence, the governing equations to be solved are (8), (9) and

$$\nabla^2 p = -\frac{1}{F^2} \nabla \cdot (\rho \hat{j}) - \nabla \cdot (\mathbf{u} \cdot \nabla) \mathbf{u} + \frac{2}{Re} \nabla^2 D - \frac{\partial D}{\partial t}, \tag{10}$$

where $D = \nabla \cdot \mathbf{u}$ must reach a steady null condition.

Because of the symmetry of the problem (see Fig. 1), there is no azimuthal dependence therefore cylindrical coordinates (z, r) in a vertical plane are used. The boundary conditions are non-slip and no flux of heat or mass through the sphere surface. Far from the sphere the velocity, pressure and stratification are due to basic state. Therefore:

- On the sphere surface:

$$(u, w) = (0, 0); \quad r \frac{\partial \rho}{\partial r} + z \frac{\partial \rho}{\partial z} = -z, \tag{11}$$

the boundary condition for pressure is obtained by substituting $u = 0$ and $w = 0$ into (8).

- On the remote boundary,

$$(u, w) = (0, 1); \quad \rho = 0, \tag{12}$$

and pressure is determined by extrapolation.

The numerical method of solution is essentially the MAC method [5] allowing for stratification [4] with density diffusion included [11].

In order to solve the flow efficiently, it is convenient to introduce the generalized curvilinear coordinates $z = z(\xi, \eta)$ and $r = r(\xi, \eta)$. The spatial derivatives are then transformed according to

$$\frac{\partial}{\partial z} = \frac{1}{J} \left(r_\eta \frac{\partial}{\partial \xi} - r_\xi \frac{\partial}{\partial \eta} \right), \quad \frac{\partial}{\partial r} = \frac{1}{J} \left(z_\xi \frac{\partial}{\partial \eta} - z_\eta \frac{\partial}{\partial \xi} \right). \tag{13}$$

Therefore, the transformed equations become

$$w_t + \frac{1}{J} \{ (ur_\eta - wz_\eta)w_\xi + (wz_\xi - ur_\xi)w_\eta \} = -\frac{(r_\eta p_\xi - r_\xi p_\eta)}{J} - \frac{\rho}{F^2} + \frac{2}{Re} \tilde{\Delta} w, \tag{14}$$

$$u_t + \frac{1}{J} \{ (ur_\eta - wz_\eta)u_\xi + (wz_\xi - ur_\xi)u_\eta \} = -\frac{1}{J} (z_\xi p_\eta - z_\eta p_\xi) + \frac{2}{Re} \left(\tilde{\Delta} u - \frac{u}{r^2} \right), \tag{15}$$

$$\rho_t + \frac{1}{J} (ur_\eta - wz_\eta)\rho_\xi + \frac{1}{J} (wz_\xi - ur_\xi)\rho_\eta = \frac{2}{Re Sc} \tilde{\Delta} \rho + (1 - w), \tag{16}$$

$$\begin{aligned} \tilde{\Delta} p = & -\frac{1}{J^2} \{ (r_\eta u_\xi - r_\xi u_\eta)^2 + (z_\xi w_\eta - z_\eta w_\xi)^2 \} + 2(z_\xi u_\eta - z_\eta u_\xi)(r_\eta w_\xi - r_\xi w_\eta) \\ & + \frac{(r_\eta u_\xi - r_\xi u_\eta + z_\xi w_\eta - z_\eta w_\xi)}{J \Delta t} - \frac{(z_\xi \rho_\eta - z_\eta \rho_\xi)}{J F^2}, \end{aligned} \tag{17}$$

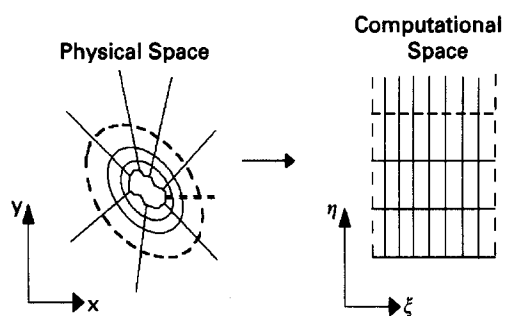


Fig. 2. Transformation process.

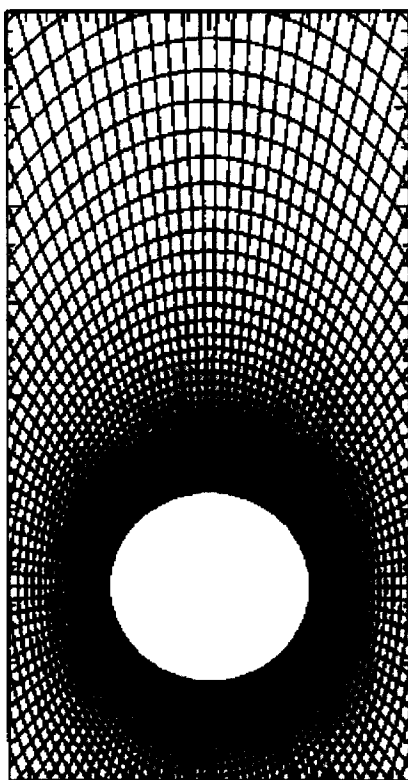


Fig. 3. Computational grid near the sphere in physical space.

where the subscripts denote differentiation with respect to that variable and the operator $\tilde{\Delta}$ is defined by

$$\tilde{\Delta}A = \frac{(\alpha A_{\xi\xi} - 2\beta A_{\xi\eta} + \gamma A_{\eta\eta})}{J^2} + \frac{1}{J^3} \{ (\alpha z_{\xi\xi} - 2\beta z_{\xi\eta} + \gamma z_{\eta\eta})(r_{\xi}A_{\eta} - r_{\eta}A_{\xi}) \} + (\alpha r_{\xi\xi} - 2\beta r_{\xi\eta} + \gamma r_{\eta\eta})(z_{\eta}A_{\xi} - z_{\xi}A_{\eta}).$$

The Jacobian of the transformation, J , and the metrics α, β and γ are given by

$$\begin{aligned} J &= z_\xi r_\eta - z_\eta r_\xi, & \alpha &= z_\eta^2 + r_\eta^2, \\ \beta &= z_\xi z_\eta - r_\eta r_\xi, & \gamma &= z_\xi^2 + r_\xi^2. \end{aligned}$$

Fig. 2 shows a sketch of the transformation process. The finite-difference equations are obtained by discretizing the set of equations (13)–(16), these equations are solved using the successive over-relaxation (SOR) method at each time step until a steady state condition, typically 25 sphere diameters, is attained. The time increment was $\Delta t = 0.0025$.

3. Grid generation

In order to generate the grid a discrete variational formulation (DV) is used. In this formulation, three properties of the grid are controlled: the spacing between the grid lines (F_s), the area of the grid cells (F_a), and the orthogonality of the grid lines (F_o). The grid is generated directly by solving a minimization problem resulting from a weighted combination of the three functionals (F_s, F_a, F_o):

$$\text{minimize } F = AF_s + BF_a + CF_o, \quad (18)$$

where A, B and C are the scaling factors. This problem is solved using a conjugate gradient iterative method, Castillo [2]. Fig. 3 shows a view of the grid obtained by this method and used as the domain of computations.

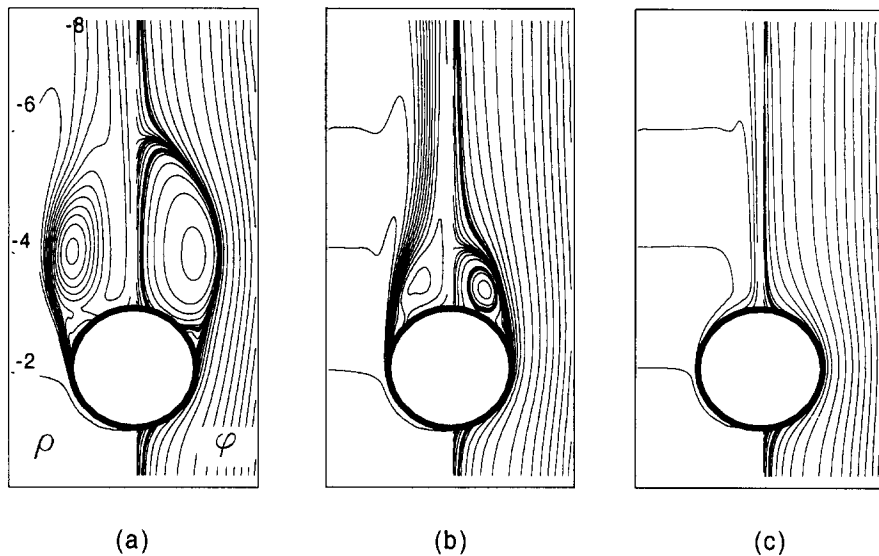


Fig. 4. Density field (left side) and stream function (right side) as function of the Re and Ri numbers.

4. Results and discussion

Fig. 4 shows the density field for $Re = 1000$ at various F numbers (200, 20, 2). As expected at $F = 200$ (weak stratification, Fig. 4a) the fluid resembles the homogeneous case; the recirculating zone, length of the bubble and angle of separation of the boundary-layer agree very well with that observed in homogeneous fluids [9, 10]. When the stratification is increased ($F = 20$), the above pattern is gradually inhibited and the separation point shifts to the rear pole (Fig. 4b). When stratification is further increased, normal velocities are strongly inhibited and thus a narrower wake is observed (Fig. 4c). It appears that the baroclinic term forces the isopycnals to remain nearly parallel to the sphere all the way to the pole and working against the viscous term in producing vorticity.

Fig. 5 shows the surface pressure corresponding to the above cases; a decreasing pressure is observed near the rear pole as stratification becomes stronger. These low levels of pressure are associated with accelerating fluid particles in the boundary-layer region. The additional input of energy to overcome the weak adverse pressure gradient is supplied by buoyancy forces.

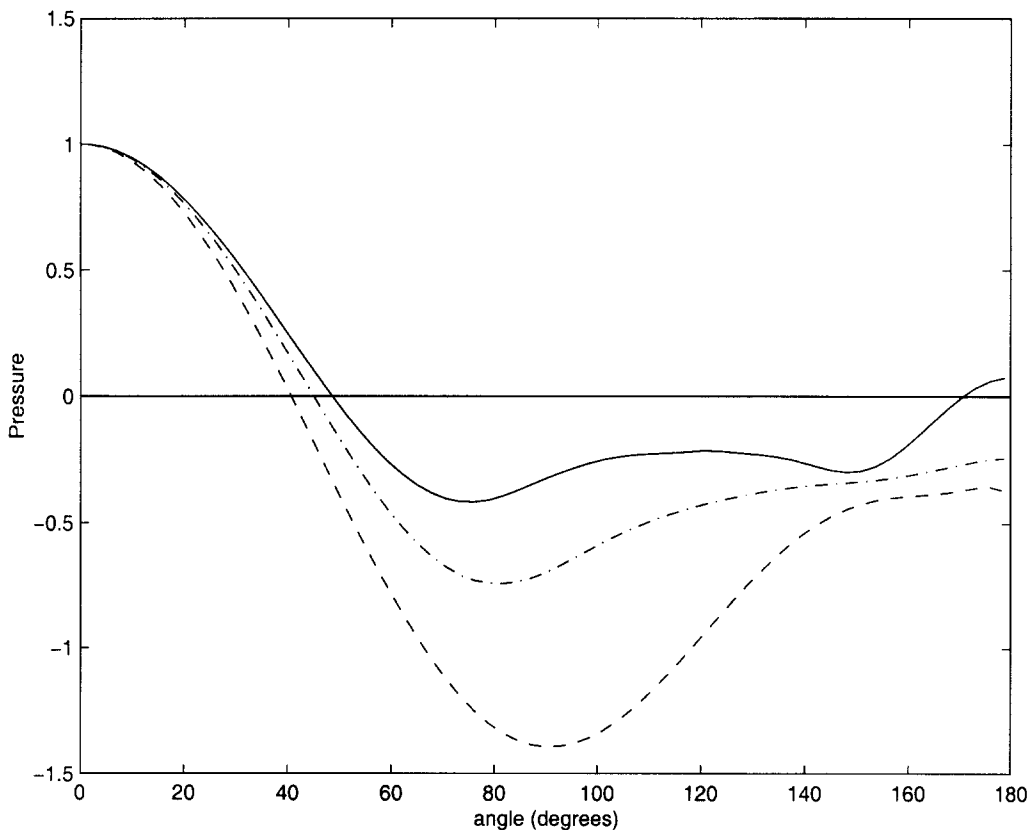


Fig. 5. Surface pressure. $F = 200$, continuous line; $F = 20$, dash-dotted line; $F = 2$, dashed line.

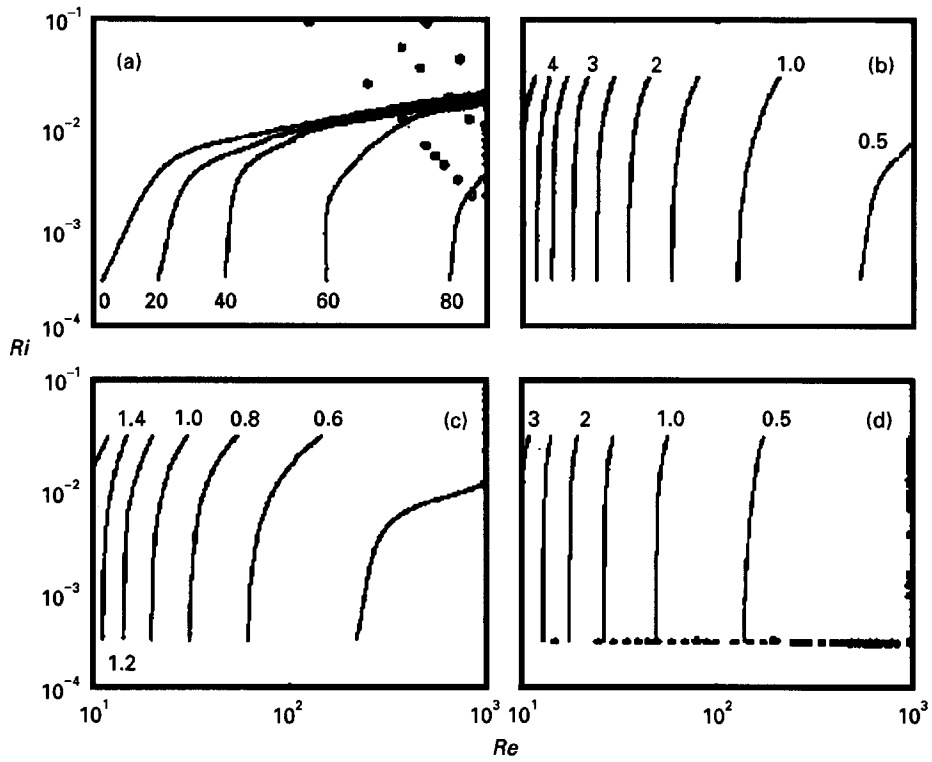


Fig. 6. Separation angles and drag coefficients in the parameter space Ri vs. Re .

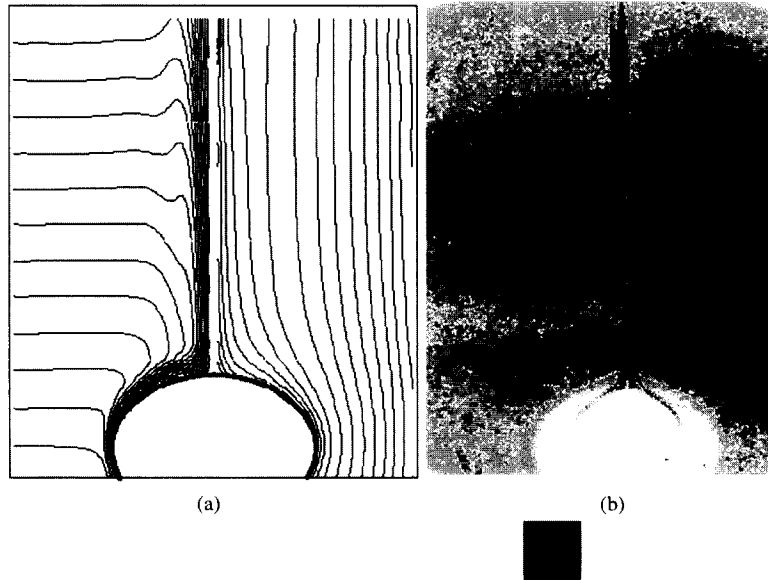


Fig. 7. Jet behind the sphere (a) isopycnals and stream function; (b) observations.

Fig. 6 presents separation angles and drag coefficients in the parameter space Ri vs. Re for the numerical experiments in this study. The dependence of the separation angle on the strength of stratification is clear (Fig. 6a). A slightly increase in the values for the drags, in comparison with the homogeneous case, is also observed (Fig. 6c and d).

The vanishing of the recirculating zone and vortices behind the sphere are characteristic of the observations [8] and are reproduced in this calculation (Fig. 7).

5. Conclusions

Stratification inhibits the BL separation, this in turn reduces the effect on the overall flow of the vorticity generated on the sphere surface. Also, the baroclinic term works against the viscous term in generating vorticity. All these combined effects make the approach to the potential flow case as Re increases and F decreases (see Fig. 4c).

Additional work should be done in order to determine the position of the BL separation in first order perturbation approximations, that is to say, to find the position where the along surface pressure gradient reverses sign, which is a necessary condition for separation [1, 3, 12]. Once the stratification produces the collapse of the vortex, this necessary condition for BL separation persists, but is not sufficient and the separation does not occur. This is the only physical example that we know, where such a situation happens.

6. Acknowledgements

To Ana Tijiboy for reading an earlier version of the manuscript. This study was supported by Universidad Autónoma de Baja California grant (4031). Partial support for computer use was provided by CONACYT under grant 1002-T9111.

References

- [1] G.K. Batchelor, *An Introduction to Fluid Dynamics*, Cambridge University Press, Cambridge, 1967.
- [2] J.E. Castillo, A discrete variational grid generation method, *SIAM J. Sci. Statist. Comput.* 12 (2) (1991) 454–468.
- [3] S. Goldstein, On laminar boundary-layer flow near a position of separation, *Q. J. Mech. Appl. Math.* 1 (1948) 43–69.
- [4] H. Hanazaki, A numerical study of three-dimensional stratified flow past a sphere, *J. Fluid Mech.* 192 (1988) 393–419.
- [5] F.H. Harlow, J.E. Welch, Numerical calculation of time-dependent viscous incompressible flow of fluid with free surface, *Phys. Fluids* 8 (1965) 2182–2189.
- [6] M.J. Lighthill, *Waves in Fluids*, Cambridge University Press, Cambridge, 1978.
- [7] D.E. Mowbray, S. H. Rarity, The internal wave pattern produced by a sphere moving vertically in a density stratified liquid, *J. Fluid Mech.* 30 (1967) 489–495.
- [8] J.L. Ochoa, M.L. Van Woert, Flow visualization of boundary layer separation in a stratified fluid, Unpublished Manuscript, Scripps Institution of Oceanography, 1977, pp. 28.
- [9] H. Schlichting, *Boundary-Layer Theory*, 6th ed., McGraw-Hill, New York, 1968.

- [10] R.I. Taneda, Experimental investigation of the wake behind a sphere at low Reynolds numbers, *J. Phys. Soc. Japan* 11 (1956) 1104–1108.
- [11] C.R. Torres, On the behavior of spheres in stratified fluids. Ph.D. thesis (in Spanish), Centro de Investigacion Cientifica y de Educaci3n Superior de Ensenada, Ensenada, B.C., M3xico, 1997, 103 pp.
- [12] J.C. Williams, III Incompressible boundary-layer separation, *Ann. Rev. Fluid Mech.* 9 (1977) 113–144.